

Optical fields of the lowest modes in a uniformly active thin subwavelength spiral microcavity

Elena I. Smotrova,^{1,*} Trevor M. Benson,² Phillip Sewell,²
Jiří Ctyroky,³ Ronan Sauleau,⁴ and Alexander I. Nosich^{1,5}

¹Institute of Radio-Physics and Electronics NASU, Kharkov 61085, Ukraine

²George Green Institute for Electromagnetics Research, University of Nottingham, Nottingham NG7 2RD, UK

³Institute of Photonics and Electronics ASCR v.v.i., 182 51 Prague 8, Czech Republic

⁴IETR, Université de Rennes 1, Rennes Cedex 35042, France

⁵Université Européenne de Bretagne, c/o Université de Rennes 1, Rennes Cedex 35042, France

*Corresponding author: elena.smotrova@gmail.com

Received May 21, 2009; revised November 6, 2009; accepted November 6, 2009;
posted November 6, 2009 (Doc. ID 111725); published December 2, 2009

A numerical study is presented of several lowest in frequency modes in a spiral microlaser. The modes in an arbitrarily shaped active cavity are considered as solutions to the two-dimensional eigenproblem for the Muller boundary-integral equations. After discretization using the Nyström-type algorithm, the eigenvalues are found in terms of frequency and material-gain threshold. © 2009 Optical Society of America
OCIS codes: 140.0140, 140.3290, 140.3410, 140.5960, 230.5750.

A serious drawback of circular microdisk lasers is the low directionality of light emission [1]. The improvement of directionality needs a distortion of cavity shape from the circle. Here, a promising device is the spiral microcavity laser [2–5]; however there is still no engineering rule to follow in its design. An accurate simulation might produce such a rule; however, this is an extremely challenging cavity shape because it combines two different scales: smooth deviation of spiral from the large-radius circle and a small, albeit abrupt, step. This makes the popular “billiard theory” impractical, and hence a full-wave numerical study is mandatory. Such a study can be based on the boundary-integral-equation (BIE) techniques; however, in this case the way of handling the cavity contour becomes crucial, a point that is not always realized by researchers. Additionally, some forms of BIEs like those used in [6–8] are contaminated with false eigenvalues [9]. This makes them unsuitable for the analysis of high- Q whispering gallery like modes.

In this Letter, we analyze the modes in a *uniformly active* spiral-shaped two-dimensional (2D) dielectric microcavity. Various recent trends in the linear optical modeling of microlasers were reviewed in [1]. Direct characterization of lasing can be achieved by introducing the macroscopic gain γ as the *active* imaginary part of the complex-valued refractive index ν_i in the *active region* (if the time dependence is $e^{-i\omega t}$, then $\nu_i = \alpha_i - i\gamma$, where $\alpha_i, \gamma > 0$) and looking for the discrete real values of k and γ as eigenvalues ($k = \omega/c$, with c being the light velocity). Such a *lasing eigenvalue problem* has been applied to the one-dimensional analysis of vertical-cavity surface-emitting lasers [10] and 2D analyses of single [11] and more complicated [12–14] microdisk lasers; for a discussion on bridging the gap between passive (pump off) and active (pump on) cavities, see [14].

In two dimensions, two polarizations can be treated separately, with the aid of either the E_z or the

H_z field component. The problem is reduced to two coupled equations known as Muller’s BIEs,

$$\begin{aligned} \varphi(\vec{r}) + \int_L A(\vec{r}, \vec{r}') \varphi(\vec{r}') dl' - 2\eta_e(\eta_i + \eta_e)^{-1} \\ \times \int_L B(\vec{r}, \vec{r}') \theta(\vec{r}') dl' = 0, \quad \vec{r} \in L, \end{aligned} \quad (1)$$

$$\begin{aligned} \theta(\vec{r}) + \int_L C(\vec{r}, \vec{r}') \varphi(\vec{r}') dl' - 2\eta_e(\eta_i + \eta_e)^{-1} \\ \times \int_L D(\vec{r}, \vec{r}') \theta(\vec{r}') dl' = 0, \end{aligned} \quad (2)$$

where $\varphi(\vec{r})$ and $2\eta_e\theta(\vec{r})/(\eta_i + \eta_e)$ are the limit values of the field function and its normal derivative, respec-

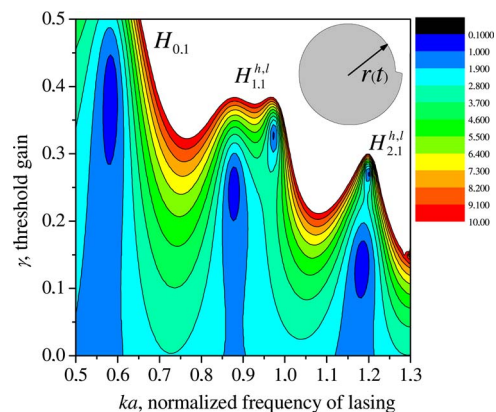


Fig. 1. (Color online) Relief of the absolute value of the determinant in the plane (ka, γ) : $d = 2.0a$, $\beta = \pi/100$, $\alpha_i = 2.63$, $\alpha_e = 1$, number of knots is $N = 100$.

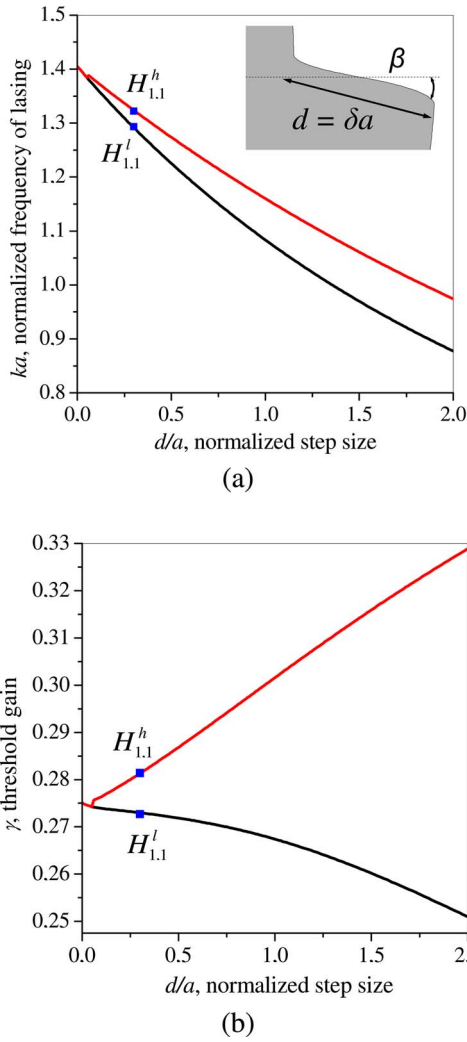


Fig. 2. (Color online) Dependences of (a) lasing frequencies and (b) thresholds of two modes of the $H_{1,1}^{h,l}$ doublet on the step size, $\beta = \pi/100$, $\alpha_i = 2.63$, $\alpha_e = 1$, and $N = 100$.

tively, if approaching the boundary L from inside; $\eta_{i,e} = \nu_{i,e}^{-1}$ (H polarization) or $\eta_{i,e} = 1$ (E polarization), with $\nu_e = 1$; d_l' is the elementary arc along L ; and the kernels A , B , C , and D are the combinations of the uniform-media Green's functions $G_{i,e}(R) = (i/4)H_0^{(1)} \times (k \nu_{i,e} R)$, where $R = |\vec{r} - \vec{r}'|$, and their first and second derivatives [15].

Together, Eqs. (1) and (2) form a Fredholm second-kind operator equation that guarantees the convergence and the controlled accuracy of numerical solutions. Additionally, they are free from false zero-threshold eigenvalues that are met for non-Muller-type BIEs, such as those used in [6–8]. Unlike [15], where integral Eqs. (1) and (2) were projected to the trigonometric polynomials, here we build a discrete model using the Nyström method. We separate the logarithmic parts from the kernels A and D and approximate the integrals with two different quadrature rules for the regular and singular parts using an equidistant set of knots (see [[16], p. 67]). Proper handling of kernel functions leads to convergent and efficient algorithms [17]. We obtain a determinantal

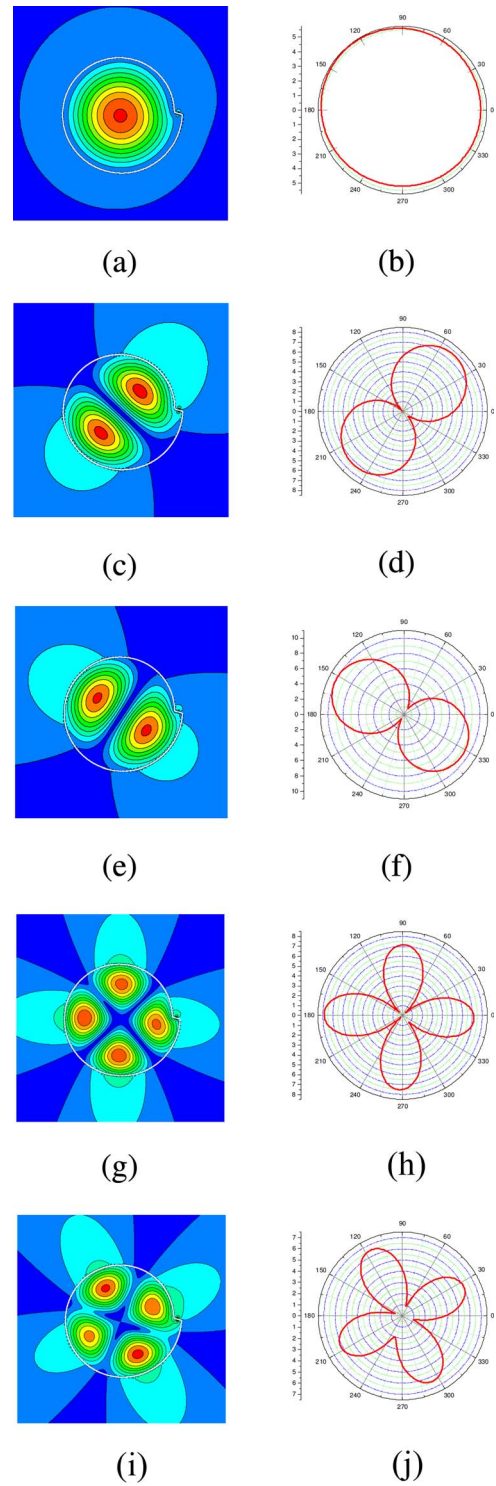


Fig. 3. (Color online) Near- and far-field patterns for the spiral-cavity modes. (a),(b) $H_{0,1}$, $ka = 0.82$, $\gamma = 0.35$; (c),(d) $H_{1,1}^h$, $ka = 1.32$, $\gamma = 0.28$; (e),(f) $H_{1,1}^l$, $ka = 1.29$, $\gamma = 0.26$; (g),(h) $H_{2,1}^h$, $ka = 1.69$, $\gamma = 0.18$; (i),(j) $H_{2,1}^l$, $ka = 1.70$, $\gamma = 0.21$. Other parameters are $d = 0.3a$, $\beta = \pi/100$, $\alpha_i = 2.63$, $\alpha_e = 1$, and $N = 50$.

equation for eigenvalues and use a secant-type iterative method [8] to find them numerically.

To consider a spiral-shaped 2D microcavity (Figs. 1 and 2), we characterize its boundary with a continuous function proposed in [18]: $L = \{r(t)\cos t, r(t)\sin t\}$, with

$$r(t) = \begin{cases} 1 - \delta/4\pi[(2\pi - \beta)/\beta t - \pi/\beta^2 t^2 - \pi], & t \in [0, \beta) \\ 1 + \delta/4\pi[(2\pi - \beta)/\beta(2\pi - t) - \pi/\beta^2(2\pi - t)^2 + \pi], & t \in (2\pi - \beta, 2\pi] \\ 1 + \delta/4\pi t, & t \in [\beta, 2\pi - \beta] \end{cases} . \quad (3)$$

Here, a is the spiral radius, $\delta=d/a$ is the normalized spiral step size, and β is the step tilt angle from the x axis. Note that the second derivative of Eq. (3) has finite jumps at $t=\beta$ and $2\pi-\beta$. This limits the accuracy assessable within reasonable time to several digits if $ka < 10$.

The initial guesses for the search of eigenvalues are found from the study of the determinant as a function of ka and γ . A typical example of such a function is presented in Fig. 1 and shows the splitting of modes owing to the loss of circular symmetry. Except for the “monopole” mode $H_{0,1}$, all other modes form doublets with higher and lower thresholds, $H_{m,n}^{h,l}$, because they originate from the twice-degenerate modes of a circular cavity. Besides, if the step size is increased the $H_{m,1}^l$ -mode threshold decreases monotonically (Fig. 2). The corresponding near- and far-field patterns are displayed in Fig. 3. They demonstrate the effect of a small step ($d=0.3a$) on the five lowest-frequency modes of a sub-wavelength cavity. Although the lowest modes do not have whispering gallery mode (WGM) properties and thus possess high thresholds, they can be interesting because a reduction in the threshold can be achieved by collecting the cavities into a cyclic photonic molecule [13]. We emphasize that, in contrast to conventional wisdom, the modes in the spiral cavity never resemble any sort of “clockwise” and “anticlockwise” waves traveling along the rim. Instead, they are always the standing waves, and the same should obviously be true for the higher-index modes, which display WGM features.

This work was supported by the National Academy of Sciences of Ukraine (NASU) via project 09/36-H and the Young Scientist Scholarship to E. I. Smotrova; the Ministry of Education and Science, Ukraine via project M/146–2009; the Royal Society,

UK via project IJP-2007/R1-FS; the Academy of Sciences of the Czech Republic, jointly with NASU, via an exchange program; and the Ministry of Education and Research, France via Research and Training Network project.

References

1. A. I. Nosich, E. I. Smotrova, S. V. Boriskina, T. Benson, and P. Sewell, *Opt. Quantum Electron.* **39**, 1253 (2007).
2. M. Kneissl, M. Teepe, N. Miyashita, and N. M. Johnson, *Appl. Phys. Lett.* **84**, 2485 (2004).
3. T. Ben-Messaoud and J. Zyss, *Appl. Phys. Lett.* **86**, 241110 (2005).
4. A. Tulek and Z. V. Vardeny, *Appl. Phys. Lett.* **90**, 161106 (2007).
5. C.-M. Kim, J. Cho, J. Lee, S. Rim, S. H. Lee, K. R. Oh, and J. H. Kim, *Appl. Phys. Lett.* **92**, 131110 (2008).
6. T.-Y. Kwon, S.-Y. Lee, M. S. Kurdoglyan, S. Rim, C.-M. Kim, and Y.-J. Park, *Opt. Lett.* **31**, 1250 (2006).
7. J. Wiersig and M. Hentschel, *Phys. Rev. A* **73**, 031802 (2006).
8. M. Hentschel and T.-Y. Kwon, *Opt. Lett.* **34**, 163 (2009).
9. D. Wilton, *Electromagnetics* **12**, 287 (1992).
10. V. O. Byelobrov and A. I. Nosich, *Opt. Quantum Electron.* **39**, 927 (2007).
11. E. I. Smotrova, A. I. Nosich, T. Benson, and P. Sewell, *IEEE J. Sel. Top. Quantum Electron.* **11**, 1135 (2005).
12. E. I. Smotrova, A. I. Nosich, T. M. Benson, and P. Sewell, *Opt. Lett.* **31**, 921 (2006).
13. E. I. Smotrova, A. I. Nosich, T. Benson, and P. Sewell, *IEEE Photon. Technol. Lett.* **18**, 1993 (2006).
14. E. I. Smotrova, J. Ctyroky, T. Benson, P. Sewell, and A. I. Nosich, *J. Opt. Soc. Am. A* **25**, 2884 (2008).
15. S. V. Boriskina, P. Sewell, T. Benson, and A. I. Nosich, *J. Opt. Soc. Am. A* **21**, 393 (2004).
16. D. Colton and R. Kress, *Inverse Acoustic and Electromagnetic Scattering Theory* (Springer, 1998).
17. J. L. Tsalamengas, *IEEE Trans. Antennas Propag.* **55**, 3239 (2007).
18. D. Kouznetsov and J. Moloney, *J. Opt. Soc. Am. B* **19**, 1259 (2002).